Automated EEG-based Screening of Depression Using Deep Convolutional Neural Network

U Rajendra Acharya , Shu Lih Oh , Yuki Hagiwara , Jen Hong Tan , Hojjat Adeli , D P Subha

PII: S0169-2607(18)30149-4
DOI: 10.1016/j.cmpb.2018.04.012
Reference: COMM 4679

To appear in: *Computer Methods and Programs in Biomedicine*

Received date: 30 January 2018
Revised date: 27 March 2018
Accepted date: 17 April 2018

Please cite this article as: U Rajendra Acharya , Shu Lih Oh , Yuki Hagiwara , Jen Hong Tan , Hojjat Adeli , D P Subha , Automated EEG-based Screening of Depression Using Deep Convolutional Neural Network, *Computer Methods and Programs in Biomedicine* (2018), doi: 10.1016/j.cmpb.2018.04.012

Highlights

- Classification of normal and depression using EEG signals
- Employed a 13-layer deep convolutional neural network model
- Minimum hand-crafted features required in this work
- Obtained accuracy of 93.54% using the left hemisphere EEG data
- Obtained accuracy of 95.49% using the right hemisphere EEG data

Automated EEG-based Screening of Depression Using Deep Convolutional Neural Network

U Rajendra Acharya[a,b,c,*], Shu Lih Oh[a], Yuki Hagiwara[a], Jen Hong Tan[a], Hojjat Adeli[d], D P Subha[e]

[a]Department of Electronics and Computer Engineering, Ngee Ann Polytechnic, Singapore.
[b]Department of Biomedical Engineering, School of Science and Technology, Singapore University of Social Sciences, Singapore.
[c]Department of Biomedical Engineering, Faculty of Engineering, University of Malaya, Malaysia.
[d]Departments of Neuroscience, Neurology, Biomedical Engineering, Biomedical Informatics, and Civil, Environmental, and Geodetic Engineering, The Ohio State University, 470 Hitchcock Hall, 2070 Neil Avenue, Columbus, OH, United States.
[e]Department of Electrical Engineering, National Institute of Technology Calicut, India.
[*]Postal Address: Department of Electronics and Computer Engineering, Ngee Ann Polytechnic, Singapore 599489.
Telephone: +65 6460 6135; Email Address: aru@np.edu.sg

Abstract

In recent years, advanced neurocomputing and machine learning techniques have been used for Electroencephalogram (EEG)-based diagnosis of various neurological disorders. In this paper, a novel computer model is presented for EEG-based screening of depression using a deep neural network machine learning approach, known as Convolutional Neural Network (CNN). The proposed technique does not require a semi-manually-selected set of features to be fed into a classifier for classification. It learns automatically and adaptively from the input EEG signals to differentiate EEGs obtained from depressive and normal subjects. The model was tested using EEGs obtained from 15 normal and 15 depressed patients. The algorithm attained accuracies of 93.5% and 96.0% using EEG signals from the left and right hemisphere, respectively. It was discovered in this research that the EEG signals from the right hemisphere are more distinctive in depression than those from the left hemisphere. This discovery is consistent with recent research and revelation that the depression is associated with a hyperactive right hemisphere. An exciting extension of this research would be diagnosis of different stages and severity of depression and development of a Depression Severity Index (DSI).

Keywords – convolutional neural network, deep learning, depression, EEG, electroencephalogram.

1. INTRODUCTION

Depression is a mental illness often correlated with loss of interest, guilt feeling, low self-esteem, poor concentration, and in the worst case, having suicidal thoughts [1]. It is graded as mild, moderate, or severe depending on the severity of the symptoms. It is estimated that roughly more than 300 million people of all ages suffer from depression worldwide [2]. Depression can be treated with psychotherapy or medical prescription if diagnosed properly but remains a persisting health issue in the society as it often goes undiagnosed [2].

A schematic comparison of synapses from a healthy subject and a depressed patient is presented in Figure 1. Neurons in depressed subjects do not function properly resulting in decreased release of neurotransmitter and a smaller concentration of receptors in synapse compared with healthy subjects [3]. Electroencephalograph (EEG) is an effective and recognized tool to record the activity of the brain [4]. It has been used extensively in recent years to study and diagnose various neurological disorders including epilepsy [5, 6, 7], seizure prediction [8, 9], the Alzheimer's disease [10], Mild Cognitive Impairment (MCI) [11], Parkinson's disease [12, 13], Creutzfeld -Jakob Disease [14], sleep studies [15, 16], schizophrenia [17], analysis of emotional states [18], and Brain-Computer Interfaces (BCI) [19, 20].

EEG is the preferred diagnostic tool in this research as it is non-invasive, economical, and easy to operate whereas the Magnetic Resonance Imaging (MRI) machine is expensive. Furthermore, the EEG records the brain's electrical activity over a period of time while the MRI machine captures the changes in blood flow of the brain within seconds to a minute. Thus, the EEG signals are used instead of MRI scans to identify depression patients. However, both normal and depressed EEG signals are chaotic and complex in nature with subtle differences reflecting different brain activities of the two groups that cannot be determined readily through visual observations. Therefore, a Computer-Aided Detection (CAD) system is proposed to diagnose depression from the EEG signals objectively. Figure 2 shows sample EEG signals of left and right hemisphere obtained from a normal subject and a person suffering from depression obtained from the Psychiatry Department of the Medical College of Calicut. Acharya et al. [21] present a review of the recent research on CAD of depression using EEG signals. The CAD system can be employed by specialists to confirm their diagnosis or by non-specialists for preliminary diagnosis.

Table 1 summarizes the various studies reported in recent years. Subha et al. [22] performed a Discrete Wavelet Transform (DWT) [23] on the EEG signals and extracted relative wavelet energy and various entropy features from the decomposed DWT coefficients. Then, these features were fed into a two-layer feedforward Artificial Neural Network (ANN) classifier to characterize EEG signals into normal and depression conditions with a reported accuracy of 98.11% for detecting depression.

Ahmadlou et al. [4] presented a wavelet-chaos methodology for the investigation of the frontal brain of patients diagnosed with Major Depressive Disorder (MDD). They explored two different measures of nonlinearity and complexity: Higuchi's and Katz's Fractal Dimension (HFD and KFD) [24]. KFDs and HFDs of the frontal lobes in the EEG sub-bands and full-band of healthy subjects and MDD are compared to determine the ones with the largest disparities between the two classes. Then, the FDs are inputted to the Enhanced Probabilistic Neural Network (EPNN) classifier of Ahmadlou and Adeli [25]) to distinguish the MDD from healthy subjects. They report the model can diagnose MDD with an accuracy of 91.3%. Subsequently, Ahmadlou et al. [26] developed a novel nonlinear approach for the investigation of brain dynamics based on the relative convergence of EEGs of different loci, called Spatio-Temporal Analysis of Relative Convergence (STARC) of EEGs and used it to investigate the difference in pathophysiology and brain dynamics in male and female MDD patients.

Hosseinifard et al. [27] analyzed the effectiveness of extracting nonlinear features from depression and normal EEG signals. The nonlinear features extracted were subjected to feature selection and subsequently fed into a logistic regression classifier for the categorization of normal and depression classes. Faust et al. [28] decomposed the EEG signals using wavelet packet decomposition [29] and extricated entropy features. Student's t-test was used to determine highly distinctive features for classification. The selected features were classified using the Probabilistic Neural Network (PNN) classifier which yielded an accuracy of 98.20% and 99.50% for the left and right hemispheres, respectively.

Acharya et al. [30] investigated the following nonlinear methods for EEG-based diagnosis of depression: Detrended Fluctuation Analysis (DFA), Fractal Dimension (FD), Higher Order Spectra (HOS), Hurst's Exponent (H), Largest Lyapunov Exponent (LLE), Recurrence Quantification Analysis (RQA), and Sample Entropy (SampEnt). The features extracted are ranked arranged according to their significance using the t-value and were inputted into 5 different classifiers. They report Support Vector Machine (SVM) [8, 31] provides the best diagnostic evaluation with an average accuracy of about 98%. Moreover, they propose a Depression Diagnosis Index (DDI) using a combination of the non-linear features. Mumtaz et al. [32] also used the SVM classifier to differentiate normal and depression EEG signals with selected clinical features extracted from the EEG signals. Liao et al. [33] employed the kernel eigen-filter-bank common spatial pattern and Principal Component Analysis (PCA) [34] to extract depression features from the EEG signals and SVM [35] for classification. They report a diagnostic accuracy of 81.23%. Recently, Bairy et al. [36] developed an EEG-based CAD system for diagnosis of depression based on a Linear Predictive Coding (LPC) methodology that uses HOS parameters to extract significant features for classification. They report sensitivity, specificity, and accuracy of 91.46%, 97.45%, and 94.30%, respectively.

In all aforementioned studies, features have to be selected using some sort of nonlinear analysis and then a machine learning classification algorithm is applied such as SVM, PNN, or EPNN. Feature selection is normally performed by trial-and-error through numerical

experimentation to achieve accurate results that can be time-consuming. In this paper, a new model is presented for EEG-based detection of depression using a deep neural network machine learning approach, known as Convolutional Neural Network (CNN). The proposed technique does not require a hand-crafted set of features to be fed into a classifier for classification. It learns automatically and adaptively from the input EEG signals to characterize depressed and normal EEG signals. The deep neural network has been the subject of significant research in recent years, in particular, image recognition [37-39]. More recently, it has been applied to a host of other problems including early diagnosis of Alzheimer's disease [40], differentiation of early-stage Creutzfeld -Jakob disease from rapidly progressive dementia [14], estimation of concrete compressive strength [41], crack damage detection in concrete surfaces [42], asphalt pavement crack detection [43], structural damage detection [44], damage assessment of high-rise building structures [45], and medical imaging field [46-50].

In a recent article, some of the authors of this paper presented a deep CNN for the automated identification of seizure using EEG signals [51]. They designed a 13-layer CNN model to automatically classify normal, pre-ictal, and ictal/seizure EEG signals [51]. High sensitivity and specificity of 95% and 90% were reported, respectively, based on 300 EEG signals, a large data set. Moreover, some of the authors have employed CNN in previous studies using Electrocardiogram (ECG) signals to diagnose various cardiac disorders [52-56]. In these studies, authors have obtained high diagnostic performances (more than 90%) even with noisy ECG signals. Based on prior experience with other biological signals, the same 13-layer CNN model is employed in this research.

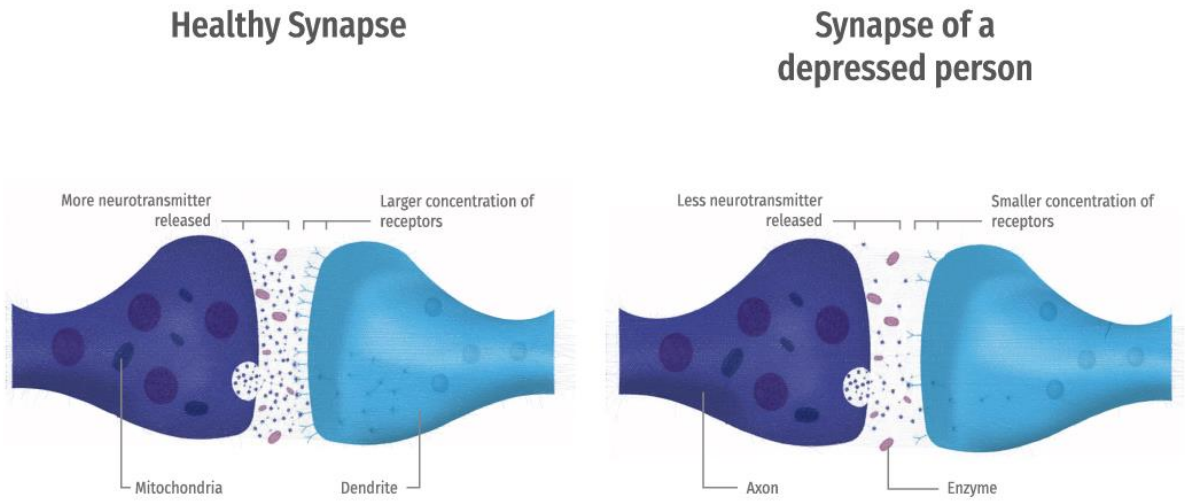

Figure 1: A schematic comparison of synapses of a healthy subject and a depressed patient (adapted from a purchased image from https://www.123rf.com/).

Table 1: A list of published works on the CAD of depression using EEG signals.

Authors	Year	Database/Techniques	Classifier Used	Performance (%)		
				Accuracy	Sensitivity	Specificity
Subha et al. [22]	2012	- 15 normal and 15 depressed subjects - DWT - Relative wavelet energy - Entropy features	ANN	98.11	98.73	97.50
Ahmadlou et al. [4]	2012	- 12 normal and 12 depressed subjects - Wavelet-chaos technique - Nonlinear features - Feature selection	Enhanced-PNN	91.30	-	-
Ahmadlou et al. [26]	2013	- 11 male and 11 female depressed subjects - STARC	Enhanced-PNN	It is reported that there is a notable difference between the EEG signals of the sexes with depression		
Hosseinifard et al. [27]	2013	- 45 normal and 45 depressed patients - Nonlinear features - Feature selection	Logistic regression	90.05	-	-
Faust et al. [28]	2014	- 15 normal and 15 depressed subjects - Wavelet packet decomposition - Entropy features - Feature selection	PNN	Left: 98.20 Right: 99.50	Left: 97.10 Right: 99.20	Left: 99.40 Right: 99.70
Acharya et al. [30]	2015	- 15 normal and 15 depressed subjects - Nonlinear features - Feature selection - Developed a depression diagnosis index	SVM	98.00	97.00	98.50
Mumtaz et al. [32]	2017	- 30 normal and 33 depressed subjects - Clinical features - Feature selection	SVM	98.40	96.66	100.00
Liao et al. [33]	2017	- 20 normal and 20 depressed subjects - Kernel eigen-filter-bank common spatial pattern - Principal component analysis	SVM	81.23	-	-
Bairy et al. [36]	2017	- 15 normal and 15 depressed subjects - Linear prediction coding	Bagged tree	94.30	91.46	97.45
Present work	2018	- 15 normal and 15 depressed subjects - 13-layer CNN	CNN	Left: 93.54 Right: 95.96	Left: 91.89 Right: 94.99	Left: 95.18 Right: 96.00

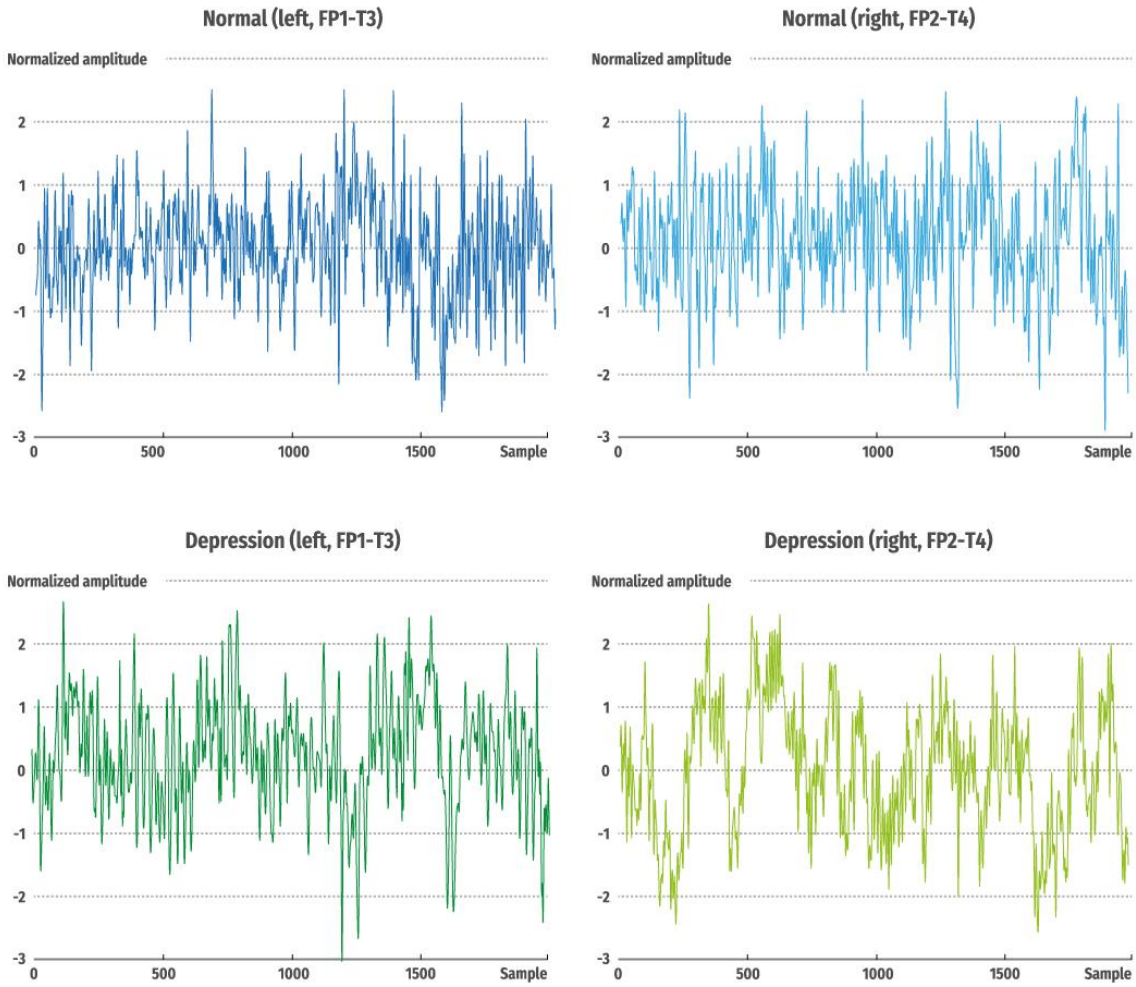

Figure 2: Sample normal and depressive EEG signals obtained from the Psychiatry Department of the Medical College of Calicut.

2. MATERIALS AND DATA

The EEG signals were obtained from the Psychiatry Department, Medical College, Calicut, Kerala, India. The EEG data collected for this study is approved by the ethics committee consisting of senior physicians. Data were obtained with a written consent form from every single participating subject.

A total of 15 normal (20 to 50 years old) and 15 depressed (20 to 50 years old) subjects were involved in the collection of data. The bipolar EEG signals were recorded from left half (FP1-T3 channel pairs) and right half (FP2-T4 channel pairs) of the brain each subject for a duration of 5 minutes with eyes open and closed (resting state). The sampling rate of the EEG signals was

maintained at 256 Hz with a notch filter of 50 Hz to eliminate power line interference. The artifacts caused by the movements of muscles and eyes twitching were removed from the EEG signal manually by an experienced neurophysiologist. The dataset used in this work includes a total of 4,348 records from 15 depressed and 15 normal subjects obtained from the left and right brain hemispheres of each group (2,174 normal and 2,174 depressed patients).

The clinical diagnosis was made by psychiatrists through asking specific questions and physical examination. Clinically diagnosed depressed patients were not classified in terms of severity.

3. METHOD

3.1 **Pre-processing**

Each record consisting of 2,000 sampling points is normalized using the Z-score normalization to overcome the amplitude scaling problem and remove the offset effect before being used for training and subsequent testing of the proposed CNN model.

3.2 CNN Architecture

A CNN has three types of layers: (i) convolution, (ii) pooling, and (iii) fully-connected [57]. In this study, the CNN model is made up of 5 convolutional layers, 5 pooling layers, and 3 fully-connected layers shown in Figure 3. The filter is a weighted vector used for convolving the input and gets adjusted during training. The filter for the convolution and pooling operations are set at 5 and 2, respectively. Filters of 5 and 2 are selected because they provided the most accurate results. Also, the stride (number of sampling point window is shifted in each operation) is fixed at 1 and 2 for the convolution and pooling operations to be explained shortly, respectively. The parameters in Table 1 are obtained through trial-and-error by optimizing the accuracy of the model.

(i) Convolutional layer: In this layer, the convolution is performed by sliding the kernel over the input to obtain a convolved output (feature map) using the following equation:

$$c_m = \sum_{n=0}^{N-1} f_n k_{m-n} \quad (1)$$

where k, f, c, and N denote signal, filter, output, and the number of data points in k, respectively. The subscript n indicates the n^{th} element of the filter vector while m corresponds to the m^{th} output element that is being calculated. As n runs from 0 to N-1, the sample fn is multiplied by the sample from the input signal k_{m-n}. These products are summed to produce the output.

The purpose of the convolutional layer is to obtain significant features from the input EEG signal for training the algorithm. The leaky rectifier linear unit (LeakyRelu) [58, 59] is applied after the convolution operation. It is employed as the activation function for layers 1, 3, 5, 7, 9, 11, and 12. The main function of LeakyRelu is to maintain the robustness of the algorithm by being more sensitive to the noise present in the EEG signals. Layer 13 uses the softmax function as the activation function.

(ii) Pooling layer: This layer decreases the size of the feature map while at the same time preserving the significant features. A max-pooling operation is employed in this study, that is, only the largest value within the stride 2 window of the feature map is retained after every max-pooling operation.

(iii) Fully-connected layer: This layer connects every neuron within the layer to every neuron in the next layer using the following equation

$$x_i = \sum_j w_{ji} y_j + b_i \qquad (2)$$

where w and b denote the weights and biases, y represents the output from the previous layer while x is the output of the current layer. Furthermore, outputs from the last fully connected layer are fed into softmax function to predict the class by determining the class probability of each EEG signals as being normal or depressive.

In this work, a 13-layer CNN model, shown in Figure 3, is employed with the number of neurons in each layer, filter size, and stride summarized in Table 2. A convolution operation is performed in the input layer with a filter size of 5 (stride 1) to obtain the 1st layer (output neurons of 1996 x 5). Then a max-pooling operation is performed in the first layer to reduce the number of neurons to 998 x 5 in layer 2. After which, another round of convolution is performed to form the next layer (layer 3). The max-pooling operation is once again applied after the convolution to obtain layer 4 with 497 x 5 neurons. Similarly, 3 more convolution and max-pooling operations are performed alternately to produce layers 5, 6, 7, 8, 9, and 10. Layer 10 is connected to 80 neurons in the first fully-connected layer, layer 11, which is in turn connected to 40 full-connected neurons in layer 12. Lastly, layer 12 is connected to the final layer with 2 outputs neurons that represents normal and depressed.

Table 2 Parameters of the CNN architecture (for both left and right hemisphere records).

Layers	Type	Number of neurons	Filter size	Stride
0-1	Convolution	1996 x 5	5	1
1-2	Max-pooling	998 x 5	2	2
2-3	Convolution	994 x 5	5	1
3-4	Max-pooling	497 x 5	2	2
4-5	Convolution	493 x 10	5	1
5-6	Max-pooling	246 x 10	2	2
6-7	Convolution	242x 10	5	1
7-8	Max-pooling	121 x 10	2	2
8-9	Convolution	117x 15	5	1
9-10	Max-pooling	58 x 15	2	2
10-11	Fully-connected	80	-	-
11-12	Fully-connected	40	-	-
12-13	Fully-connected	2	-	-

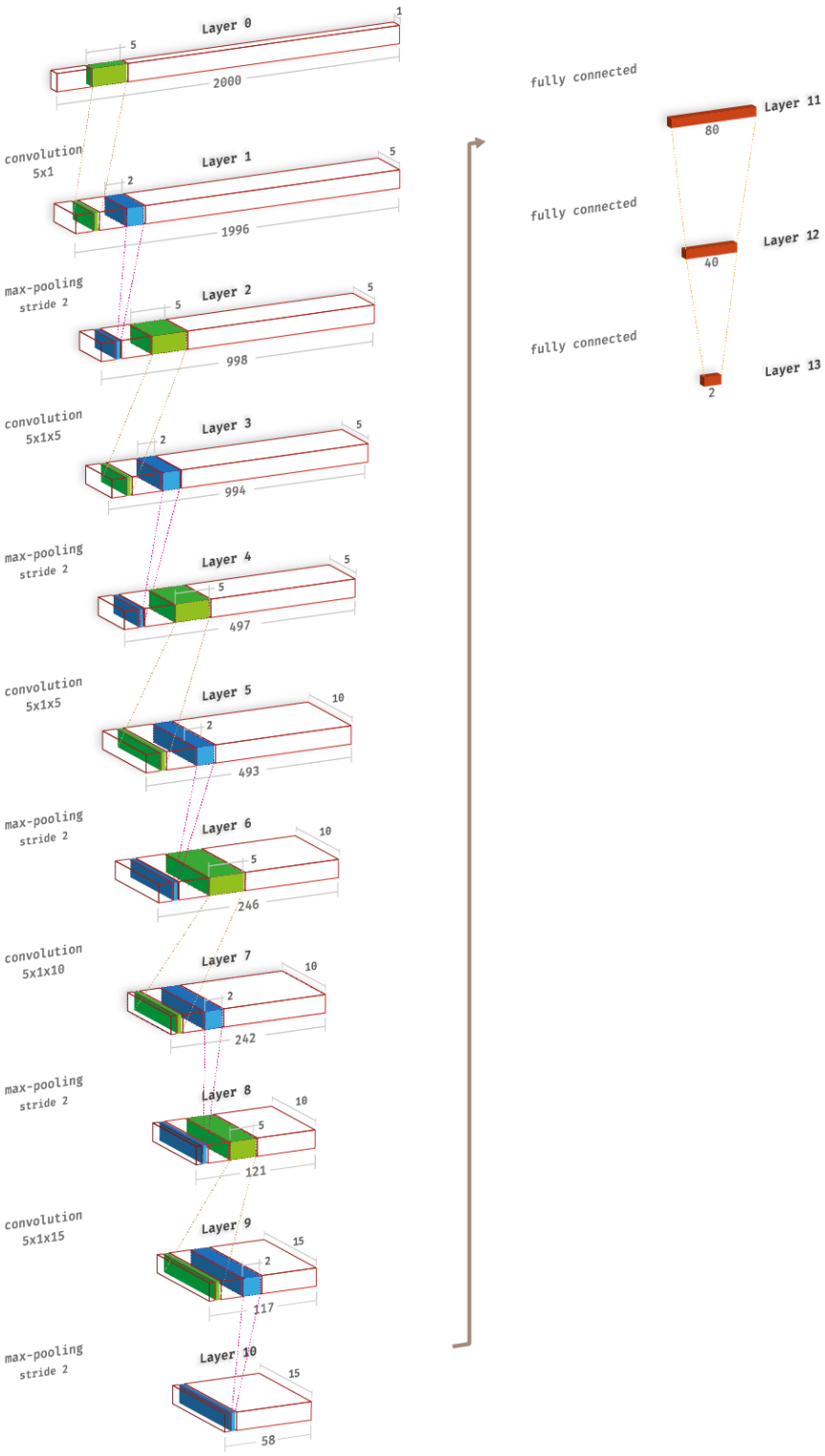
Layer 0
1
5
2000
convolution
5x1
Layer 1
5
2
1996
max-pooling
stride 2
Layer 2
5
5
998
convolution
5x1x5
Layer 3
5
2
994
max-pooling
stride 2
Layer 4
5
5
497
convolution
5x1x5
Layer 5
10
2
493
max-pooling
stride 2
Layer 6
10
5
246
convolution
5x1x10
Layer 7
10
2
242
max-pooling
stride 2
Layer 8
10
5
121
convolution
5x1x15
Layer 9
15
2
117
max-pooling
stride 2
Layer 10
15
58
fully connected
Layer 11
80
fully connected
Layer 12
40
fully connected
Layer 13
2

Figure 3: The architecture of the proposed CNN model.

3.3 Training

The network is trained using the backpropagation algorithm [60] with a batch size (the number of training samples in an iteration) of 5. An optimization algorithm, adaptive moment estimation (Adam) [61] is adopted in this work to update the parameters of the proposed network structure. It was observed it enables the network to converge at a fast rate thereby improving the efficiency of the training process.

The following equation is used to update the 1st moment estimate [61]. All operations on vectors are element-wise.

$$m_t = \beta_1 m_{t-1} + (1-\beta_1)\left[\frac{\partial c}{\partial \theta}\right]_t \quad (3)$$

where m, t, c, θ_t and $\frac{\partial c}{\partial \theta}$ are defined as the 1st moment vector, timestep, cost function, resulting parameters (weights), and gradient, respectively. The parameters β_1 and β_2 represent the exponential decay rates which are chosen to be 0.9 and 0.999 respectively [61].

The following equation is used to update the 2nd moment estimate [61].

$$v_t = \beta_2 v_{t-1} + (1-\beta_2)\left[\frac{\partial c}{\partial \theta}\right]_t^2 \quad (4)$$

The following equations are used to compute the 1st and 2nd moment estimates respectively [61].

$$\hat{m}_t = \frac{m_t}{1-\beta_1^t} \quad (5)$$

$$\hat{v}_t = \frac{v_t}{1-\beta_2^t} \quad (6)$$

In addition, the following equation is used to update the weights of links connecting the layers [61].

$$\theta_t = \left[1 - \frac{\alpha\lambda(1-\beta_1)}{\sqrt{\hat{v}_t}+\epsilon}\right]\theta_{t-1} - \frac{\alpha\hat{m}_t}{\sqrt{\hat{v}_t}+\epsilon} \quad (7)$$

where α and ϵ denote the learning rate and numerical value and are set at 1x10-4 and 10-8 respectively in this work. The variable λ, known as regularization parameter, is also one of the essential parameters during training to prevent data overfitting. It is tuned to 0.2 in this work.

To avoid overfitting and improve the generalization, the dropout [62] technique is applied to the fully-connected layers 11 and 12. During training for each mini-batch, some of the neurons from these layers are selected randomly and dropped. This forces the model to learn from a subset of input features and not the entire input features. The rate is set to 0.9. i.e. a probability of 90% a neuron will be kept and a probability of 10% that a neuron will be dropped out during the training.

The proposed CNN model is trained using 90% of the EEG dataset. The remaining 10% of the dataset is used to test the model.

3.4 Testing

The model is tested using a ten-fold cross-validation [63] strategy using the test dataset (10% of the EEG data). The testing of the proposed model is repeated 10 times. Then, an overall performance is computed by averaging the results from all 10 iterations.

4 RESULTS

The proposed network was trained and tested on a computer with 2 Intel Xeon (2.40 GHz processor) with a 24 GB RAM. It required approximately 199.07 seconds to finish an epoch of training on the left hemisphere data and 198.68 seconds to finish one epoch of training on the right hemisphere data.

The performances (accuracy, sensitivity, and specificity) obtained for each fold using the left and right EEG data are summarized in Tables A1 and A2, respectively. Figures 4 and 5 show the data in those tables and the variations of performance over the ten folds for the left and right hemisphere, respectively.

The results obtained using the left and right hemisphere data are recorded in Tables 3 and 4, respectively. Using the EEG data obtained from the left hemisphere, 4.8% of the normal EEG signals is misclassified as depressive EEG signals and 8.1% of the depressive signals is wrongly categorized as normal EEG signals (Table 3). Using the EEG data obtained from the

right hemisphere (Table 4), 4.0% of the signals are misclassified as depressive class and roughly 5.0% of the depressive EEG signals is misclassified as the normal class.

The overall average classification results are presented in Table 5. It includes the average diagnostic performances obtained using the proposed CNN model and the number of correctly identified and wrongly identified normal and depressive EEG signals. A high classification performance (> 90%) is achieved for all three parameters of sensitivity, specificity, and accuracy in both the left and right hemisphere EEG data.

Table 3: Confusion matrix for left hemisphere data (performance across all 10-folds).

		Predicted				
		Normal	**Depression**	***Accuracy* (%)**	***Sensitivity* (%)**	***Specificity* (%)**
Original	**Normal**	2,055	104	93.54	95.18	91.89
	Depression	175	1,984	93.54	91.89	95.18

Table 4: Confusion matrix for right hemisphere data (performance across all 10-folds).

		Predicted				
		Normal	**Depression**	***Accuracy* (%)**	***Sensitivity* (%)**	***Specificity* (%)**
Original	**Normal**	2,087	87	95.49	96.00	94.99
	Depression	109	2,065	95.49	94.99	96.00

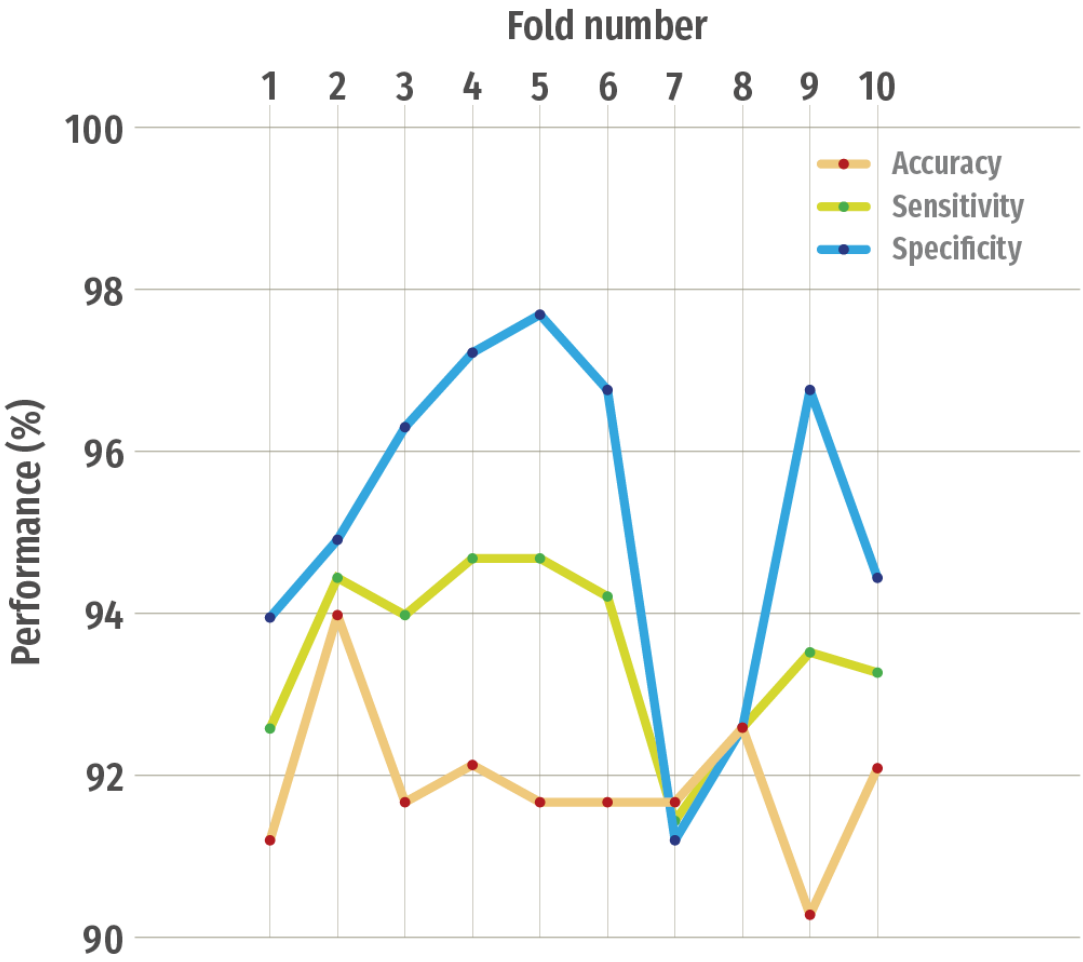

Figure 4 Performance for each fold using the left hemisphere EEG data.

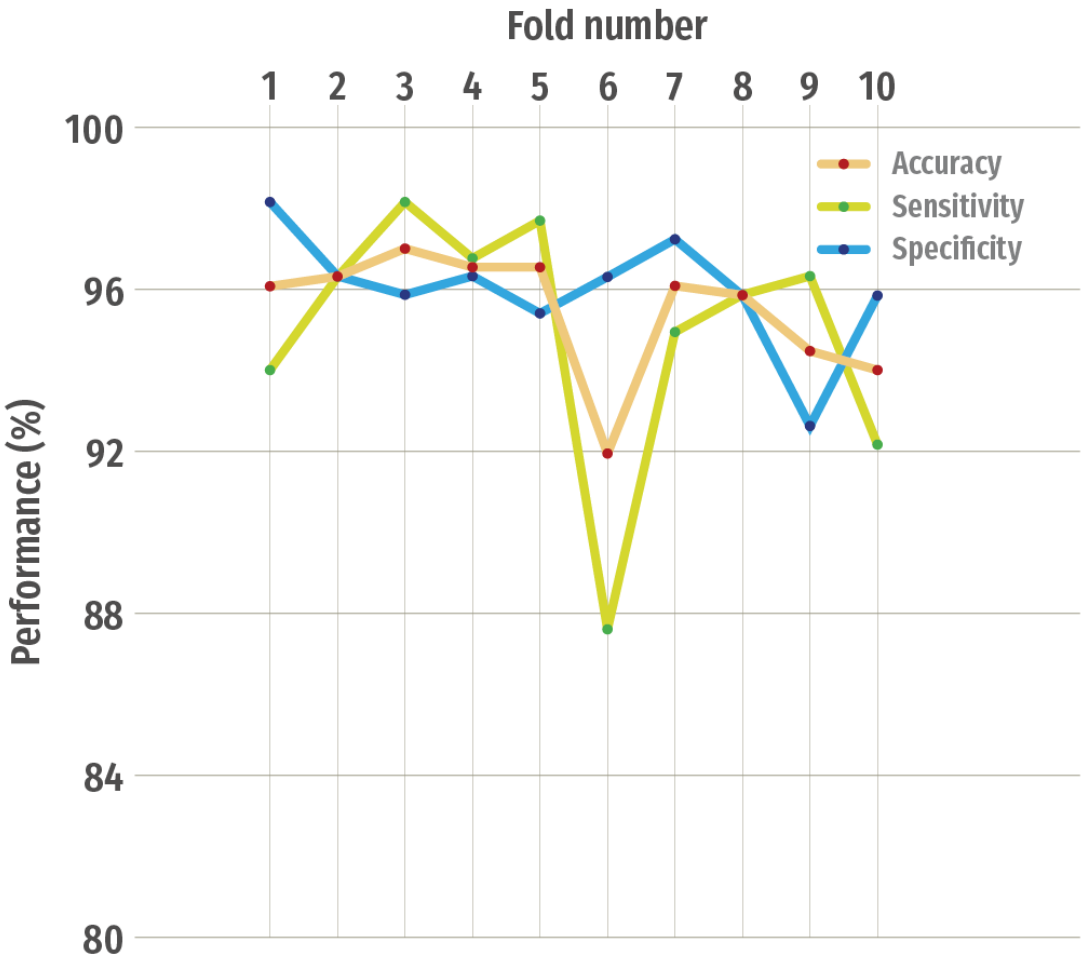

Figure 5 Performance for each fold using the right hemisphere EEG data.

Table 5: Overall classification results for left and right hemisphere EEG data.

	T_P	T_N	F_P	F_N	*Accuracy* (%)	*Sensitivity* (%)	*Specificity* (%)
Left	1,984	2,055	104	175	93.54	91.89	95.18
Right	2,065	2,087	87	109	95.49	94.99	96.00

T_P = true positive T_N = true negative F_P = false positive F_N = false negative

5 DISCUSSION

Table 1 summarizes various works published on the computer-aided diagnosis of depression using EEG data. These works employed conventional neural network or machine

learning classifiers using various feature extraction techniques such as clinical features [32], entropies [22, 28], nonlinear features [4, 26, 27, 30], statistical analysis [36], and relative wavelet energy [22]. After the extraction of features, these studies often employed feature reduction and selection approaches to select the most discriminative features to feed into a classifier. In contrast, the novelty of the proposed CNN is that it does not require the employment of feature extraction, selection, and reduction. The model has the ability to self-learn and pick up distinctive features during training without a separate feature extraction or feature selection step. This is indeed an advantage of the proposed model.

Even though this study is based a limited number of EEG signals obtained from 30 subjects (15 normal and 15 depression subjects), the proposed algorithm achieved an accuracy of 93.54% and 95.96% from the left and right hemisphere, respectively, without the use of a semi-manually-selected set of features to differentiate the two normal and depression classes.

The proposed CNN model can be implemented in a clinical setting to be used as a tool for objective diagnosis of depression using EEG signals. In the current clinical practice, the diagnosis of depression is based on questionnaires and the physical emotions displaced by the patients. Furthermore, the proposed diagnosis system can be installed as a web-based application to be used by non-specialist clinicians remotely. Once the EEG signals are obtained from the patients, they will be sent to the servers (located in the hospitals) in the cloud where the proposed CNN model can be used to make the diagnosis. The diagnosis can be sent immediately to the clinic. (see Figure 6).

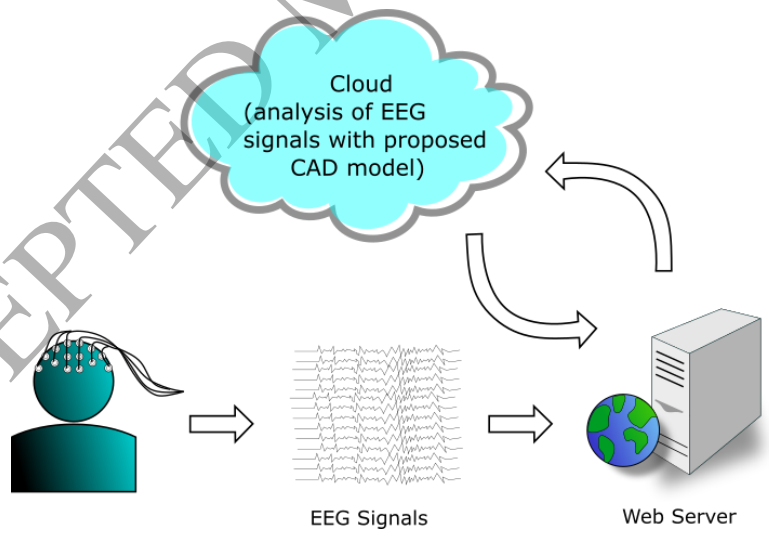

Figure 6 An illustration of the implementation of the proposed system into a clinical setting.

6 CONCLUSION

The paper presented the first application of the deep neural network concept and CNN for diagnosis of depression. The proposed CNN model does not require the semi-manually-selected extraction and selection of features for classification. Rather, the model can self-learn and pick up distinct features during the training of the algorithm. In this work, the algorithm attained a high accuracy of 93.5% and 96.0% using EEG signals from the left and right hemisphere, respectively. Based on the results obtained using the proposed model with a limited number of EEG data, it can be concluded that the CNN model can be used for computer-assisted diagnosis of depression rather reliably. Moreover, this proposed algorithm can serve as a second-opinion to validate the diagnosis made by a clinician. Nonetheless, the analytical performance of the proposed model can be improved with a larger set of EEG signals obtained from the left or right hemisphere.

In this research, it was discovered that the EEG data from the right hemisphere yields higher performance in terms of sensitivity, specificity, and accuracy compared with data from the left hemisphere. Hence, it can be concluded that the EEG signals from the right hemisphere are more distinctive in depression than the EEG signals obtained from the left hemisphere [28]. This is consistent with recent research and revelation that the depression is associated with a hyperactive right hemisphere [59].

Finally, the proposed algorithm can be extended to diagnose different stages and severity of depression as well as other neurological disorders. A key to successful application in the clinical setting would be the collection of the necessary data to train the model.

7 REFERENCES

1. World Federation for Mental Health, Depression: a global crisis, Occoquan, VA, USA, (2012).
2. World Health Organization, Depression, obtained from http://www.who.int/mediacentre/factsheets/fs369/en/, 2017.
3. National Institute of Mental Health, Brain basics, obtained from https://www.nimh.nih.gov/health/educational-resources/brain-basics/brain-basics.shtml#GrowingBrain.
4. M. Ahmadlou, H. Adeli, A. Adeli, Fractality analysis of frontal brain in major depressive disorder, International Journal of Psychophysiology 85 (2012) 206-211.
5. Cogan, J. Birjandtalab, M. Nourani, J. Harvey, V. Nagaraddi, Multi-biosignal analysis for epileptic seizure monitoring, International Journal of Neural Systems 27 (1) (2017) 1650031 (18 pages).

6. C. Geier, K. Lehnertz, Which brain regions are important for seizure dynamics in epileptic networks? Influence of link identification and EEG recording montage on node centralities, International Journal of Neural Systems 27 (1) (2017) 1650033 (14 pages).
7. L. Guo, Z. Wang, M. Cabrerizo, M. Adjouadi, A cross-correlated delay shift supervised learning method for spiking neurons with application to interictal spike detection in epilepsy, International Journal of Neural Systems 27 (3) (2017) 1750002 (19 pages).
8. B. Direito, C. A. Teixeira, F. Sales, M. Castelo-Branco, A. Dourado, A realistic seizure prediction study based on multiclass SVM, International Journal of Neural Systems 27 (3) (2017) 1750006 (15 pages).
9. Y. Varatharajah, R. K. Iyer, B. M. Berry, G. A. Worrel, B. H. Brinkmann, Seizure forecasting and the preictal state in canine epilepsy, International Journal of Neural Systems 27 (1) (2017) 1650046 (12 pages).
10. F. C. Morabito, M. Campolo, D. Labate, G. Morabito, L. Bonanno, A. Bramanti, S. de Salvo, A. Marra, P. Bramanti, A longitudinal EEG study of Alzheimer's disease progression based on a complex network approach, International Journal of Neural Systems 25 (2) (2015) 1550005 (18 pages).
11. N. Mammone, L. Bonanno, S. de Salvo, S. Marino, P. Bramanti, A. Bramanti, F. C. Morabito, Permutation disalignment index as an indirect, EEG-based, measure of brain connectivity in MCI and AD patients, International Journal of Neural Systems 27 (5) (2017) 1750020 (19 pages).
12. T. J. Hirschauer, H. Adeli, J. A. Buford, Computer-aided diagnosis of Parkinson's disease using enhanced probabilistic neural network, Journal of Medical Systems 39 (11) (2015) 179.
13. R. Yuvaraj, M. Murugappan, K. Sundaraj, M. I. Omar, N. M. Ibrahim, K. Mohamad, R. Palaniappan, U. R. Acharya, H. Adeli, E. Mesquita, Brain functional connectivity patterns for emotional state classification in Parkinson's disease patients without dementia, Behavioural Brain Research 298 (2016) 248-260.
14. F. C. Morabito, M. Campolo, N. Mammone, M. Versaci, S. Franceschetti, F. Tagliavini, V. Sofia, D. Fatuzzo, A. Gambardella, A. Labate, I. Mumoli, G. G. Tripodi, S. Gasparini, V. Ciancci, C. Sueri, E. Ferlazzo, U. Aguglia, Deep learning representation from electroencephalography of early-stage Creutzfeld-Jakob disease and features for differentiation from rapidly progressive dementia, International Journal of Neural Systems 27 (2) (2017) 1650039 (15 pages).
15. J. C. Bruder, M. Duemepelmann, D. L. Piza, M. Mader, A. Schulze-Bonhage, J. Jacobs-Le Van, Physiological ripples associated with sleep spindles differ in waveform morphology from epileptic ripples, International Journal of Neural Systems 27 (7) (2017) 1750011 (15 pages).
16. A. Dereymaeker, K. Pillay, J. Vervisch, S. Van Huffel, G. Naulaers, K. Jansen, M. de Vos, An automated quiet sleep detection approach in preterm infants as a gateway to assess

brain maturation, International Journal of Neural Systems 27 (6) (2017) 1750023 (18 pages).
17. S. A. Akar, S. Kara, F. Latifoğlu, V. Bilgiç, Analysis of the complexity measures in the EEG of Schizophrenia patients, International Journal of Neural Systems 26 (2) (2016) 1650008 (13 pages).
18. Y. Tonoyan, D. Looney, D. P. Mandic, M. M. van Hulle, Discriminating multiple emotional states from EEG using a data-adaptive, multiscale information-theoretic approach, International Journal of Neural Systems 26 (2) (2016) 1650005 (15 pages).
19. R. Liu, Y. Wang, G. I. Newman, S. Ying, N. V. Thakor, EEG classification with a sequential decision-making method in motor imagery BCI, International Journal of Neural Systems 27 (8) (2017) 1750046 (16 pages).
20. A. R. Sereshkeh, R. Trott, A. Bricout, T. Chua, Online EEG classification of covert speech for brain-computer interfacing, International Journal of Neural Systems 27 (8) (2017) 1750033 (16 pages).
21. U. R. Acharya, V. K. Sudarshan, H. Adeli, J. Santhosh, J. E. W. Koh, A. Adeli, Computer-aided diagnosis of depression using EEG signals, European Neurology 73 (2015) 329-336.
22. D. P. Subha, P. K. Joseph, Classification of EEG signals in normal and depression conditions by ANN using RWE and signal entropy, Journal of Mechanics in Medicine and Biology 12 (4) (2012) 1240019-1-1240019-13.
23. H. Adeli, S. Ghosh-Dastidar, Automated EEG-based diagnosis of neurological disorders-inventing the future of neurology, CRC Press, Taylor and Francis, Boca Raton, Florida (2010).
24. F. Xu, W. Zhou, Y. Zhen, Q. Yuan, Q. Wu, Using fractal and local binary pattern features for motor imagery classification of ECOG motor imagery task obtained from the right brain hemisphere, International Journal of Neural Systems 26 (6) (2016) 1650022 (13 pages).
25. M. Ahmadlou, H. Adeli, Enhanced Probabilistic Neural Network with Local Decision Circles: A Robust Classifier, Integrated Computer-Aided Engineering 17 (3) (2010) 197-210.
26. M. Ahmadlou, H. Adeli, A. Adeli, Spatiotemporal analysis of relative convergence of EEGs reveals differences between brain dynamics of depressive women and men, Clinical EEG and Neuroscience 4 (3) (2013) 175-181.
27. B. Hosseinifard, M. H. Moradi, R. Rostami, Classifying depression patients and normal subjects using machine learning techniques and nonlinear features from EEG signal, Computer Methods and Program in Biomedicine 109 (2013) 339-345.
28. O. Faust, P. C. A. Ang, S. D. Puthankattil, P. K. Joseph, Depression diagnosis support system based on EEG signal entropies, Journal of Mechanics in Medicine and Biology 14 (3) (2014) 1450035-1-1450035-20.

29. X. Jiang, H. Adeli, Wavelet packet-autocorrelation function method for traffic flow pattern analysis, Computer-Aided Civil and Infrastructure Engineering 19 (5) (2004) 324-337.
30. U. R. Acharya, V. K. Sudarshan, H. Adeli, J. Santhosh, J. E. W. Koh, S. D. Puthankattil, A. Adeli, A novel depression diagnosis index using nonlinear features in EEG signals, European Neurology 74 (2015) 79-83.
31. H. Dai, A wavelet support vector machine-based neural network meta model for structural reliability assessment, Computer-Aided Civil and Infrastructure Engineering 32 (4) (2017) 344-357.
32. W. Mumtaz, L. Xia, S. S. A. Ali, M. A. M. Yasin, M. Hussain, A. S. Malik, Electroencephalogram (EEG)-based computer-aided technique to diagnose major depressive disorder (MDD), Biomedical Signal Processing and Control 31 (2017) 108-115.
33. S. C. Liao, C. T. Wu, H. C. Huang, W. T. Cheng, Major depression detection from EEG signals using kernel eigen-filter-bank common spatial patterns, Sensors 17 (6) (2017) 1385.
34. S. Ghosh-Dastidar, H. Adeli, N. Dadmehr, Principal component analysis - enhanced cosine radial basis function neural network for robust epilepsy and seizure detection, IEEE Transactions on Biomedical Engineering 55 (2) (2008) 512-518.
35. L. Khedher, L. A. Illan, J. M. Gorriz, J. Ramirez, A. Brahim, A. Meyer-Baese, Independent component analysis – support vector machine-based computer aided diagnosis system for Alzheimer's with visual support, International Journal of Neural Systems 27 (3) (2017) 1650050 (8 pages).
36. G. M. Bairy, S. L. Oh, Y. Hagiwara, S. D. Puthankattil, O. Faust, U. C. Niranjan, U. R. Acharya, Automated diagnosis of depression electroencephalograph signals using linear prediction coding and higher order spectra features, Journal of Medical Imaging and Health Informatics 7 (8) (2017) 1857-1862.
37. I. Arel, D. C. Rose, T. K. Karnowski, Researcher frontier: deep machine learning – a new frontier in artificial intelligence research, IEEE Computational Intelligence Magazine 5 (4) (2010) 13-18.
38. M. Koziarski, B. Cyganek, Image recognition with deep neural networks in presence of noise – dealing with and taking advantage of distortions, Integrated Computer-Aided Engineering 24 (4) (2017) 337-350.
39. F. Ortega-Zamorano, J. M. Jerez, I. Gómez, L. Franco, Layer multiplexing FPGA implementation for deep back-propagation learning, Integrated Computer-Aided Engineering 24 (2) (2017) 171-185.
40. A. Ortiz-Garcia, J. Muruilla, J. M. Gorriz, J. Ramirez, Ensembles of deep learning architectures for the early diagnosis of Alzheimer's disease, International Journal of Neural Systems 26 (7) (2016) 1650025 (23 pages).

41. M. H. Rafiei, W. H. Khushefati, R. Demirboga, H. Adeli, Supervised deep restricted boltzmann machine for estimation of concrete compressive strength, ACI Materials Journal 114 (2) (2017) 237-244.
42. Y. J. Cha, W. Choi, O. Büyüköztürk, Deep learning-based crack damage detection using convolutional neural networks, Computer-Aided Civil and Infrastructure Engineering 32 (5) (2017) 361-378.
43. A. Zhang, Y. Fei, K. C. P. Wang, B. Li, Y. Liu, J. Q. Li, C. Chen, E. Yang, X. Dai, Y. Peng, Automated pixel-level pavement crack detection on 3D asphalt surfaces using a deep learning network, Computer-Aided Civil and Infrastructure Engineering 31 (10) (2017) 805-819.
44. Y. Z. Lin, Z. H. Nie, H. W. Ma, Structural damage detection with automatic feature-extraction through deep learning, Computer-Aided Civil and Infrastructure Engineering 32 (12) (2017) 1025-1046.
45. M. H. Rafiei, H. Adeli, A novel machine learning based algorithm to detect damage in highrise building structures, The Structural Design of Tall and Special Buildings 26 (18) (2017) (DOI: 10.1002/tal.1400).
46. H. C. Shin, H. R. Roth, M. Gao, L. Lu, Z. Xu, I. Nogues, J. Yao, D. Mollura, R. M. Summers, Deep convolutional neural networks for computer-aided detection: CNN architectures, dataset characteristics and transfer learning, IEEE Transactions on Medical Imaging 35 (5) (2016) 1285-1298.
47. S. Pereira, A. Pinto, V. Alves, C. A. Silva, Brain tumor segmentation using convolutional neural networks in MRI images, IEEE Transactions on Medical Imaging 35 (5) (2016) 1240-1251.
48. N. Tajbakhsh, J. Y. Shin, S. R. Gurudu, R. T. Hurst, C. B. Kendall, M. B. Gotway, J. Liang, Convolutional neural networks for medical image analysis: full training or fine tuning?, IEEE Transactions on Medical Imaging 35 (5) (2016) 1299-1312.
49. J. H. Tan, U. R. Acharya, S. V. Bhandary, K. C. Chua, S. Sivaprasad, Segmentation of optic disc, fovea and retinal vasculature using a single convolutional neural network, Journal of Computational Science 20 (2017) 70-79.
50. J. H. Tan, H. Fujita, S. Sivaprasad, S. V. Bhandary, A. K. Rao, K. C. Chua, U. R. Acharya, Automated segmentation of exudates, haemorrhages, microaneurysms using single convolutional neural network, Information Sciences 420 (2017) 66-76.
51. U. R. Acharya, S. L. Oh, Y. Hagiwara, J. H. Tan, H. Adeli, Deep convolutional neural network for the automated detection and diagnosis of seizure using EEG signals, Computers in Biology and Medicine, https://doi.org/10.1016/j.compbiomed.2017.09.017.
52. U. R. Acharya, H. Fujita, S. L. Oh, M. Adam, J. H. Tan, K. C. Chua, Automated detection of coronary artery disease using different durations of ECG segments with convolutional neural network, Knowledge-Based Systems 946 (2017) 1-10.
53. U. R. Acharya, H. Fujita, S. L. Oh, U. Raghavendra, J. H. Tan, M. Adam, A. Gertych, Y. Hagiwara, Automated identification of shockable and non-shockable life-threatening

ventricular arrhythmias using convolutional neural network, Future Generation Computer Systems 79 (3) (2018) 952-959.

54. U. R. Acharya, H. Fujita, S. L. Oh, Y. Hagiwara, J. H. Tan, M. Adam, Application of deep convolutional neural network for automated detection of myocardial infarction using ECG signals, Information Sciences 416 (2017) 190-198.
55. U. R. Acharya, H. Fujita, S. L. Oh, Y. Hagiwara, J. H. Tan, M. Adam, Automated detection of arrhythmias using different intervals of tachycardia ECG segments with convolutional neural network, Information Sciences 405 (2017) 81-90.
56. U. R. Acharya, S. L. Oh, Y. Hagiwara, J. H. Tan, M. Adam, A. Gertych, R. S. Tan, A deep convolutional neural network model to classify heartbeats, Computers in Biology and Medicine 89 (2017) 389-396.
57. J. G. Lee, S. Jun, Y. W. Cho, H. Lee, G. B. Kim, J. B. Seo, N. Kim, Deep learning in medical imaging: general overview, Korean Journal of Radiology 18 (4) (2017) 570-584.
58. K. He, X. Zhang, S. Ren, J. Sun, Delving deep into rectifiers: Surpassing human-level performance on image net classification, IEEE International Conference on Computer Vision, Santiago, Chile, (2015).
59. D. Hecht, Depression and the hyperactive right-hemisphere, Neuroscience Research 68 (2010) 77-87.
60. S. L. Hung, H. Adeli, Parallel backpropagation learning algorithms on cray Y-MP8/864 supercomputer, Neurocomputing 5 (6) (1993) 287-302.
61. D. P. Kingma, J. L. Ba, ADAM: A method for stochastic optimization, 3rd International Conference on Learning Representations, San Diego, (2015).
62. N. Srivastava, G. Hinton, A. Krizhevsky, I. Sutskever, R. Salakhutdinov, Dropout: A simple way to prevent neural networks from overfitting, Journal of Machine Learning Research 15 (2014) 1929-1958.
63. R. O. Duda, P. E. Hart, D. G. Stork, Pattern classification 2nd edition, New York, John Wiley and Sons, (2001).

8 Appendix

Table A1: Left EEG performance for each fold.

Fold Number	Accuracy (%)	Positive Predictive Value (%)	Sensitivity (%)	Specificity (%)
1	92.58	93.81	91.20	93.95
2	94.44	94.86	93.98	94.91
3	93.98	96.12	91.67	96.30
4	94.68	97.07	92.13	97.22
5	94.68	97.54	91.67	97.69
6	94.21	96.59	91.67	96.76
7	91.44	91.24	91.67	91.20
8	92.59	92.59	92.59	92.59
9	93.52	96.53	90.28	96.76
10	93.27	94.29	92.09	94.44
Mean ± SD	**93.54 ± 1.07**	**95.06 ± 2.07**	**91.89 ± 0.96**	**95.18 ± 2.14**

SD = standard deviation

Table A2: Right EEG performance for each fold.

Fold Number	Accuracy (%)	Positive Predictive Value (%)	Sensitivity (%)	Specificity (%)
1	96.08	98.08	94.01	98.16
2	96.32	96.31	96.31	96.33
3	97.01	95.95	98.16	95.87
4	96.55	96.33	96.77	96.33
5	96.55	95.50	97.70	95.41
6	91.95	95.98	87.61	96.31
7	96.09	97.18	94.95	97.24
8	95.86	95.87	95.87	95.85
9	94.48	92.92	96.33	92.63
10	94.01	95.69	92.17	95.85
Mean ± SD	**95.49 ± 1.56**	**95.98 ± 1.32**	**84.99 ± 3.13**	**95.99 ± 1.43**

Graphical abstract